Role of Architecture on the Conformation, Rheology, and Orientation Behavior of Linear, Star, and Hyperbranched Polymer Melts. 2. Linear Viscoelasticity and Flow Birefringence

Semen B. Kharchenko[†] and Rangaramanujam M. Kannan*

Department of Chemical Engineering and Materials Science, Wayne State University, Detroit, Michigan 48202

Received September 6, 2002; Revised Manuscript Received November 13, 2002

ABSTRACT: In the preceding publication, we showed that the hyperbranched polystyrenes (HBPS) synthesized as part of this study may be viewed as starlike molecules with a high branch density, which are either unentangled or weakly entangled. In this paper, the role of architecture, especially the branch density, on the rheological and orientation behavior is investigated using simultaneous, quantitative stress and flow birefringence measurements in the melt state. Linear PS and eight-arm symmetric PS stars follow the stress−optical rule (SOR) over a wide dynamic range, with the stress−optical coefficient (C) governed by the arm molecular weight. When the branch density is "moderate" (greater than ∼20 arms), there is only a hint of nonterminal behavior in the viscoelastic moduli, while the C drops by 30% compared to a star with eight arms of comparable length. When the branch density is "high" (∼50 arms), and the arms are unentangled, the nonterminal behavior in G^* is clearly apparent, and there is a dramatic breakdown in the stress−optical rule in these homopolymer melts. The quantitative birefringence measurements suggest that the "excess" birefringence may be due to the "form" contributions from the core−shell structure. Such a structure may be formed by the preferential radial stretching of the chain segments near the core, as suggested by other studies on hyperstars. For comparable chain density, the core would be bigger than the shell when the arm length is smaller. Therefore, the 5K-HBPS exhibits a more severe breakdown compared to the 10K-HBPS.

Introduction

Recent advances in metallocene catalysis, anionic polymerization, and dendrimer synthesis have made it possible for polymer architecture to be "tunable" . As a result, a wide range of polymers with linear, comb, star, dendritic, and hyperbranched architectures have been synthesized and characterized. This has generated renewed interest in understanding the role of architecture on the viscoelastic and the processing behavior. Linear polymers and dendritic polymers may represent two ends of branching complexity. The long-time viscoelastic behavior of high molecular weight linear and star polymers are mostly governed by entanglement coupling of molecular chains and the additional topological constraints due to the branching architecture.[1,2] Yet, recent results have shown that dendritic polymers behave like Newtonian liquids. There appears to be a lack of entanglement-like response due to the geometric constraints near the surface of a dendrimer molecule. Hyperbranched polymers (HBP) are highly branched structures with less well-defined branching architecture, but can be synthesized in "one step" , thereby making them significantly cheaper than dendrimers. However, there is a significant need to characterize the topology, the associated rheology and the orientation behavior of these materials.

In the preceding paper (part 1),[3] we established the differences in molecular architecture of HBP in comparison to linear and symmetric star polymers by studying dilute solution properties of these materials. Our HBPS materials appear to be "starlike" polymers with high branch density. In this paper, we address the effect of branching architecture on the rheology and orientation behavior. Mechanical and flow birefringence responses of these homopolymer melts have been measured quantitatively and simultaneously over a wide range of temperature and shear frequency. Rheo-optical measurements of linear and symmetric star polystyrene melts with unentangled branches are used to compare and interpret the flow behavior of hyperbranched polystyrenes.

Background

Viscoelastic behavior of polymers with "relatively simple" architectures such as linear, comblike, and symmetric star have been extensively studied both theoretically and experimentally.[4−10] However, more complex architectures have received greater attention only recently.[11−15] The difference in the mechanism for relaxation of branched molecules from that of linear ones was indicated by their profoundly different viscoelastic properties in early studies.[16] Contrary to linear chains, branched polymers impose significant constraints for molecular motions realized through the existence of a permanent (chemical) cross-link, the branch point. One of the possible ways for such molecule to relax might be intuitively visualized by gradual retraction of dangling segments (or branches) toward the connector point. Reptation theory has been modified by introduction of contour-length fluctuations and constraint release to describe the relaxation process of branched polymers.[17] Milner and McLeish successfully developed a "parameter-free theory" for the stress relaxation of stars, in which only two factors were needed to accurately depict the relaxation process of the star: polymer entanglement molecular weight M_e and its monomeric friction coefficient ξ.[18] This has been

* Corresponding author. E-mail: rkannan@che.eng.wayne.edu.
† Currently at NIST, Gaithersburg, MD.

10.1021/ma025649y CCC: $25.00
Published on Web 12/28/2002

adapted and further improved by others.[19−21] Larson has developed a computational algorithm to describe the rheology of well-characterized linear, star, their mixtures as well as pompom and comb melts.[15] The model was shown to be sensitive to both degree and type of branching. The broad aspects of the theories have been supported by experiments.[9,22−24]

The effect of branching has also been viewed from the point of view of theories and experiments on long chain branching (LCB). In fact, shear and extensional rheometry was shown to be related to architectural parameters and was used in an attempt to "estimate" the degree of LCB. Even though a uniform correlation has not been established between rheology and topology for a wide variety of polymers, topology has been shown to play a crucial role.[25−28] It is possible that flow birefringence may provide another signature of the branching topology, yet birefringence of highly branched polymer melts has not been investigated in detail.

It is important to stress that, in contrast to the rheology of star polymers, the majority of experimental studies on dendrimers and hyperbranched polymers have focused on their dilute solution properties, such as intrinsic viscosity and molecular conformation.[29] Available melt rheology studies on dendrimers and hyperbranched polymers have shown that they exhibit Newtonian response, characterized by a lack of entanglements even at high total molecular weight.[30] Yet, HBP with sufficiently long branches are known to exhibit entanglement-like features[31,32] analogous to symmetric stars with entangled arms,[33−35] and polymers with long-chain branches.[25−27,36,37] Recent work by Roovers, Vlassapoulous, Pakula, and co-workers has focused on hyper-star polymers which are made by linking high molecular weight linear polymers to a dendritic core.[35,38] These highly entangled, highly branched polymers have been shown to exhibit both polymeric and colloid-like behavior. This soft-colloidal behavior was evident in the rheology, light scattering, and SAXS measurements.

In this paper, we explore how the branch length and branch density affect the rheological and orientation behavior, by investigating "nearly unentangled" symmetric star and hyperbranched polymers using the quantitative rheo-optical methods discussed below.

Methods

The quantitative and simultaneous measurements of stress and birefringence, and the application of stress−optical rule (SOR) to these homopolymer melts, form the basis for our results.[39] This rule relates corresponding components of the stress ($\boldsymbol{\sigma}$) and the birefringence ($\mathbf{n}$) tensors and is considered to work well for homopolymer melts up to very large strain rates. The proportionality constant, the stress−optical coefficient (C), is observed to be independent of frequency and slightly dependent on temperature. The SOR is given by

$$\boldsymbol{\sigma} = \mathbf{n}/\mathrm{C} \tag{1}$$

and

$$C = \frac{2\pi}{45}\frac{(n^2+2)^2(\alpha_1-\alpha_2)}{nkT} \tag{2}$$

where n is the mean refractive index, α_1 and α_2 are the polarizabilities along the backbone and perpendicular to it, respectfully, and T is temperature. Note that in the equation above, besides the polymer chemistry, it contains no factor that could account for the dependence of C on molecular architecture.

Simultaneous measurements of stress and flow birefringence were performed using a custom-built polarization-modulation rheo-optical apparatus.[40] The details about this apparatus are discussed elsewhere.[41] The actual measurements of flow birefringence is done by monitoring the retardation (δ) and its orientation angle, developed upon interaction of polarization-modulated light with the sample undergoing flow. The retardation is directly related to birefringence ($\Delta n'$):

$$\Delta n' = \delta(\lambda/2\pi\mathrm{d}) \tag{3}$$

where $\lambda = 633$ nm, and d is the path length of light in the shear sandwich. The magnitude ($|\Delta n'|$) and the orientation angle of the birefringence (χ) and the corresponding components of the stress tensor can be related to each other in the shear−shear gradient plane as described below. For small-amplitude oscillatory shear ($\gamma = \gamma_0 \sin \omega t$), the shear stress is described by

$$\sigma_{12} = \gamma_0 (G' \sin \omega t + G'' \cos \omega t) \tag{4}$$

where γ_0 is strain amplitude, ω is shear frequency, and G' and G'' are storage and loss modulus, respectively. The component of birefringence that is proportional to shear stress is

$$\mathrm{n}_{12} = \gamma_0 (B' \sin \omega t + B'' \cos \omega t) = (1/2)\Delta n' \sin(2\chi) \tag{5}$$

where B' and B'' are in-phase and out-of-phase components of n_{12}.

The stress−optical coefficient, C is calculated using:

$$C = \Delta n' \sin(2\chi)/(2\sigma_{12}) \tag{6}$$

When SOR fails, it is useful to define the normalized components of C based on the ratios of the in-phase and out-of-phase parts of n_{12} and σ_{12}:

$$C' = B'/G' \tag{7}$$

$$C'' = B''/G'' \tag{8}$$

The magnitude and the frequency dependence of C' and C'' will provide insights into the elastic and viscous contributions of the "excess" birefringence in the densely branched polymers.

Materials

Linear, symmetric star, and model hyperbranched PS used in this work are described in the preceding publication with more information provided in Table 1.

Results

HBPS melts with different branch lengths and branch densities (Table 1) appear to obey the time−temperature superposition (TTS) over a wide temperature range of 120−210 °C (Figure 1). To create a master curve, a reference temperature of 150 °C was used, with no vertical shift factors. Note that the rest of the figures in this paper are also prepared with the reference to this temperature. Previous studies observed *both* themorheological simplicity and complexity in branched polymers. From the standpoint of molecular relaxation, branched polymers may have different temperature dependencies for their relaxation, compared to linear chains. Therefore, increased activation energies for flow of LCB polymers are not uncommon.[27] Graessley proposed that the effect of branching on the temperature coefficient of viscosity would be molecular conformation sensitive, as there may be energy differences between the trans and gauche configurations.[9] Examples of the

Table 1. Stress−Optical Coefficient of Model Polystyrenes

polymer architecture	M_w, g/mol	M_n, g/mol	PDI	est f	est 10^9C (Pa^{-1})	comments (T, temp; ω, frequency
			Entangled Linear-PS			
61K-L-PS	61 800	58 300	1.06	2	−4.60	T-, ω-insensitive
1015K-L-PS	1 015 000	985 500	1.03	2	−4.55	
			Unentangled Linear-PS			
5K-L-PS	5110	4800	1.07	2	−2.60	T-sensitive, ω-insensitive
13K-L-PS	13 100	12 200	1.07	2	−3.70	
19K-L-PS	19 000	17 800	1.07	2	−4.45	
			Symmetric Stars			
3-arm-20K	61 800	57 700	1.09	3	−4.60	
8-arm-10K	74 000	71 200	1.04	8	−3.70	T-, ω-insensitive
8-arm-45K	391 000	379 600	1.03	8	−4.85	
			HBPS			
5K-HBPS	252 700	212 400	1.19	48	−1.60[a]	T-, ω-sensitive
10K-HBPS	575 600	456 800	1.26	51	−2.50[a]	
20K-HBPS	960 700	313 000	3.07	31	−3.50	T-, ω-insensitive[b]
50K-HBPS	1 264 000	730 700	1.73	20	−3.70	

[a] These values are estimated in the high-frequency regime. [b] Holds in the temperature and frequency ranges studied.

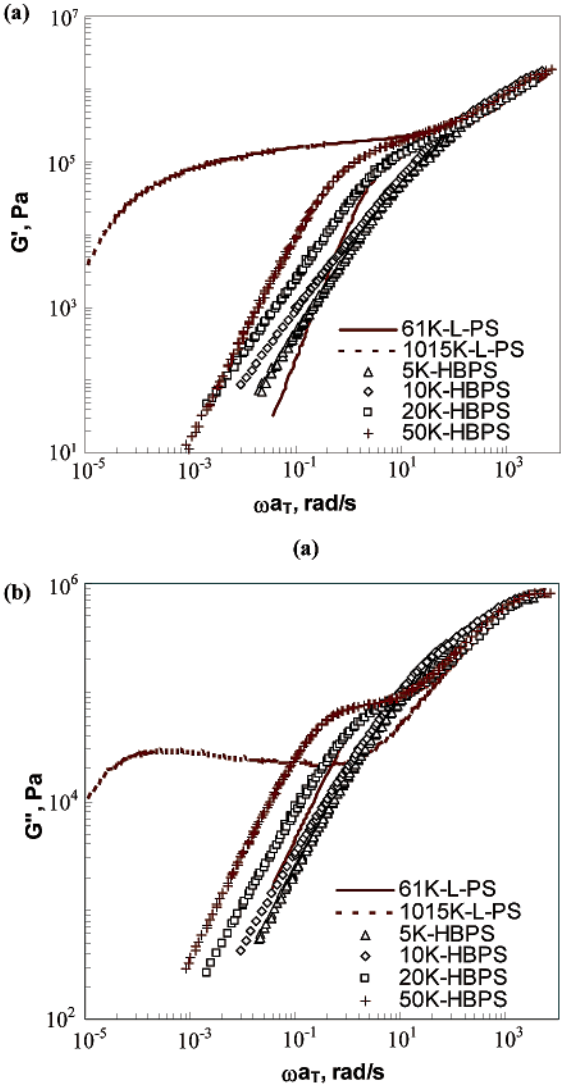

Figure 1. Development of nonterminal type of relaxation for HBPS seen in (a) $G'(\omega)$ and (b) $G''(\omega)$. Solid and dashed lines show linear unentangled and entangled polystyrenes, respectively, and symbols show HBPS.

failure of TTS were found in long-chain branched polyethylene and hydrogenated 1,2-polybutadiene, and "apparent" TTS failure was found in poly(ethylene-*alt*-propylene).[9,42] Conversely, TTS has been shown to work

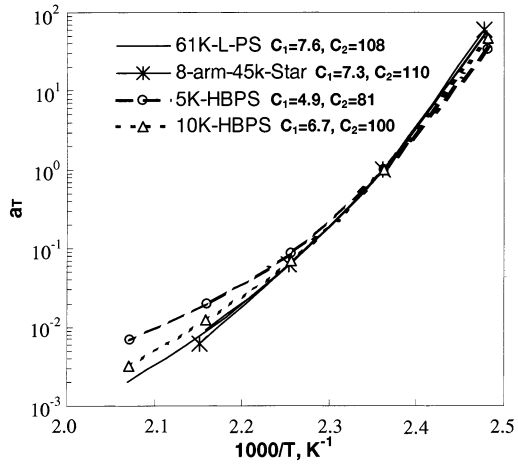

Figure 2. Effect of the molecular architecture on the temperature dependence of the horizontal shift factor a_T. Note that the fitting parameters C_1 and C_2 in WLF equation: $\log(a_T) = -C_1(T - T_{ref})/(C_2 + T - T_{ref})$, are given in the inset of the figure.

for relatively densely branched polystyrenes,[31] hyperbranched etherimidies,[43] and hyperbranched polyisobutylene.[32] It appears that the densely branched HBPS used in this study do not show the thermorheological complexity observed in some long-chain branched polymers.

The horizontal shift factor, a_T, of the highly branched HBPS has a different temperature dependence from those of L-PS (Figure 2).[41] The linear polymers and symmetric stars in the present study exhibit comparable temperature dependence of a_T, suggesting a similar coefficient of thermal expansion of free volume. Interestingly, HBPS with moderate branching density (20K-HBPS and 50K-HBPS) seem not to deviate from this dependence too (not shown). On the other hand, the HBPS with high branch density (5K-HBPS and 10K-HBPS), demonstrate appreciably weaker temperature dependence of their a_T. DSC analysis showed that the T_g's of these two polymers were comparable to those of high molecular weight L-PS (96 and 98 °C, respectively). For HBPS with shortest branches (5K-HBPS), this dependence becomes especially weak toward higher temperatures, suggesting a different coefficient of thermal expansion of free volume (α_f) for this polymer. A Williams−Landel−Ferry analysis was performed using the a_T data. Using the fitting parameters C_1 and C_2 in

the WLF equation, the coefficient of thermal expansion of free volume was calculated, with the relation $\alpha_f = 1/(2.303C_1C_2)$. The estimated value of α_f for L-PS and 8-arm-47K-star is $(5.7 \pm 1) \times 10^{-4}$ K^{-1}(Figure 2). [44−46] On the other hand, α_f for 10K-HBPS and 5K-HBPS seems to be higher and was estimated to be 6.5×10^{-4} and 10.9×10^{-4} K^{-1}, respectively (Figure 2). The larger coefficient of thermal expansion obtained for 5K-HBPS in present study is consistent with weaker temperature dependence of its horizontal shift factor (a_T).[31]

Even though several linear polymers were studied in our work, comparative viscoelastic behavior of only the 61K-L-PS and 1015K-L-PS is shown. The 61K-L-PS demonstrates familiar terminal response characteristic of homopolymer melts ($G' \sim \omega^2$, $G'' \sim \omega^1$). The 1015K-L-PS shows a well-defined plateau ($G_N^0 \sim 2 \times 10^5$ Pa), but the terminal behavior could not be captured even at the highest temperatures employed in this study. The densely branched HBPS melts (5K-HBPS and 10K-HBPS), on the other hand, exhibit nonterminal behavior, characterized by a broadening of the transition to the "terminal" region and a different terminal frequency dependence from the Rouse-like behavior of linear polymers. For 5K-HBPS, $G' \sim \omega^{1.12}$, and for 10K-HBPS, $G' \sim \omega^{1.10}$. In most of the polymers, the slope is nearly constant over more than *two decades of frequency*. Usually, the degree to which the rubbery/terminal transition broadens is strongly affected by polydispersity and branch architecture. The 50K-HBPS, which is more polydisperse (PDI = 1.73) than either 5K-HBPS (PDI = 1.19) or 10K-HBPS (PDI = 1.26) developed terminal relaxation that deviated from the Rouse prediction only weakly. Therefore, given relatively low polydispersity of 5K-HBPS and 10-K-HBPS the strongest nonterminal response of these materials is thought to have origins in high branch density (Table 1). Our results are in accord with findings, that the most evidence of the effect of polymer architecture is associated with the frequency dependence of the storage modulus $G'(\omega)$.[25,47] Notably, 20K-HBPS does seem to display nonterminal behavior, but the direct relation of this effect to branching density may not be as straightforward, for this polymer has the widest molecular weight distribution among all model polymers. However, the low molecular weight fraction in this polymer would be expected to impact the high frequency response more than the terminal response. The role of molecular architecture in the frequency dependence of loss modulus is relatively weaker (Figure 1b), with 5K-HBPS and 10K-HBPS showing terminal slopes of $G'' \sim \omega^{0.91}$ and $G'' \sim \omega^{0.85}$, respectively. Such character of linear viscoelastic behavior seen in G' and G'' may reflect the existence of additional relaxation modes arising from "structural" contributions. Apparently, these modes may exist in the present HBPS, more easily detected for polymers with the highest degree of branching density.

The dynamic moduli of HBPS, and linear PS are comparable at the high frequency end. Segmental relaxation, which governs the response of a polymer in this dynamic range, appears to be insensitive not only to the molecular weight but also to the difference in polymer architecture (Figure 1). The latter has been confirmed by a number of studies done on symmetric stars[9,48] and was likewise validated for hyperbranched polystyrene and hyperbranched polyisobutylene.[31,32] HBPS in our study, with the exception of 50K-HBPS, do not develop a plateau in the frequency response of their elastic modulus, even though their overall molecular weight is much higher than entanglement molecular weight of linear PS chain. This finding is analogous to the behavior of symmetric stars, where rheology is controlled only by the length of an arm. Similar results of Newtonian flow were found for hyperbranched polyesters both in solution and in the melt.[49,50]

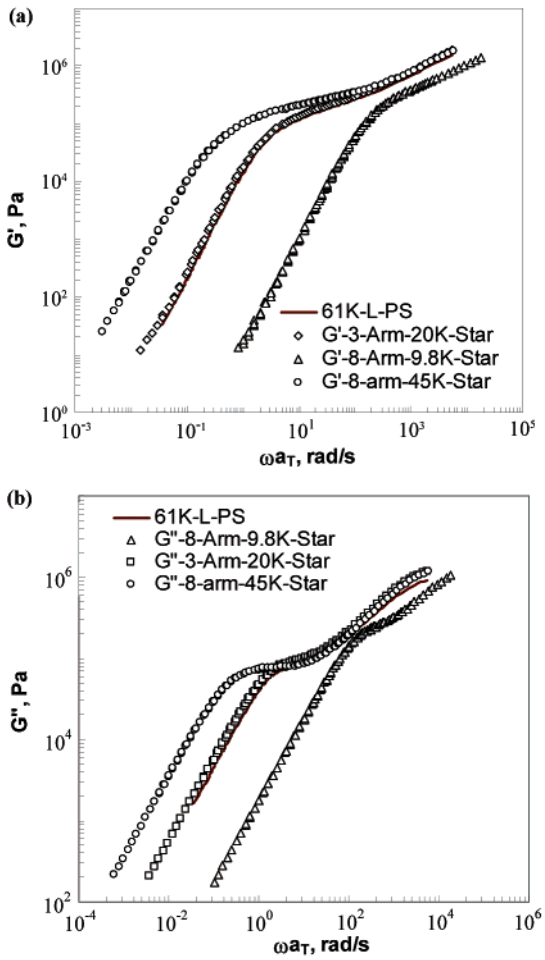

Figure 3. Rouse type of relaxation of symmetric polystyrene stars with three and eight arms seen in (a) $G'(\omega)$ and (b) $G''(\omega)$. The solid line shows weakly entangled linear PS, and symbols show PS stars.

The viscoelastic measurements suggest that the nonterminal behavior may be due to additional relaxation modes arising from the branching architecture of the starlike HBPS. To understand the role of branch density, symmetric star PS with relatively short arms and lower branch densities were investigated (Table 1). Figure 3 shows that nonterminal behavior was not observed for these polymers, i.e., both moduli developed a typical Rouse-like terminal behavior with $G' \sim \omega^2$ and $G'' \sim \omega^1$. The 50K-HBPS and the 8-arm-45K symmetric star have comparable arm molecular weight, but the 50K-HBPS has approximately 20 branches. In fact, the dynamic moduli of these two polymers are nearly identical, except for a small hint of nonterminal response in G' of the 50K-HBPS (Figure 4). This might suggest that when the number of arms (or branches) is less than ~20, the viscoelastic moduli are mostly governed by the arm molecular weight. Previous experimental works on star polymers support this concept.[9,48]

Flow Birefringence. Using the combination of simultaneous measurements of stress and birefringence,

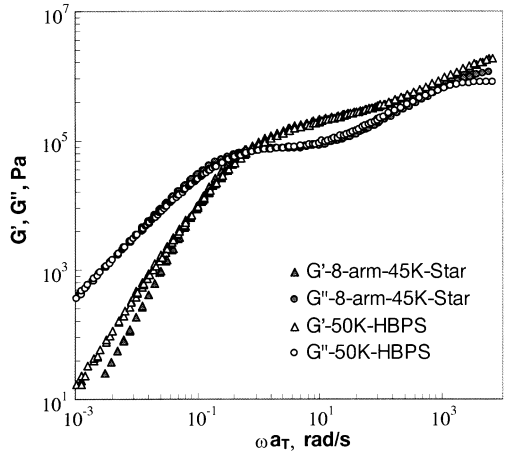

Figure 4. Starlike behavior of 50K-HBPS.

we aim to get deeper insights into the microscopic origins responsible for the dynamics of HBPS, as seen through the development of the nonterminal relaxation, their significantly different viscosity, and thermal properties.

Linear Polystyrenes. Study of the stress−optic behavior of linear polystyrenes is necessary to develop a basis for comparison. All linear polymers obeyed the stress−optical rule over the wide temperature and frequency range employed in this study. The measured stress−optical coefficient (C) was found to be nearly frequency independent for molecular weights ranging from 61 000 to 1.015×10^6 and equal to about -4.5×10^{-9} Pa^{-1} (Table 1).[41] This value agrees very well with the published literature values for linear PS evaluated in shear and extensional flows.[39,51] Weak temperature dependence of the stress−optical coefficient appears to be consistent with the theory of entropic elasticity, which predicts that, for a given amount of conformational distortion (i.e., birefringence), an increase in entropic stress is observed with an increase in absolute temperature.[10] Consequently, negative dC/dT slopes are in agreement with the theory. Interestingly L-PS with molecular weight in the range higher than the Rouse segment size (850[52]) but lower than the critical molecular weight (36 200) exhibited more complex stress−optical behavior (Table 1). Not only was the C lower, but also its dependence on temperature was totally reversed (not shown), pertaining to more complex relaxation modes. In such instances, the slowest relaxation of the polymer chain is suggested to be controlled by nonentropic, glassy contributions extended to quite large length and time scales.[53] Despite this, the SOR was still obeyed over a wide dynamic range. The transition from one type of relaxation to another is molecular weight sensitive, and linear PS of molecular weight within the range from 19 000 to 61 000 would provide an exact location of this transition. However, more detailed research in this direction is beyond the scope of the present work, and has been addressed elsewhere.[53]

Symmetric Stars and Moderately Branched HBPS. Symmetric stars with longest arms (3-arm-20K and 8-arm-47K stars) obey the SOR (Figure 5a), producing stress−optical coefficients similar to the values obtained for entangled linear polystyrenes (Figure 6a). However, lower values of C were received for 8-arm-10K-star, even though this polymer has the same number of arms (but of a lower molecular weight) as

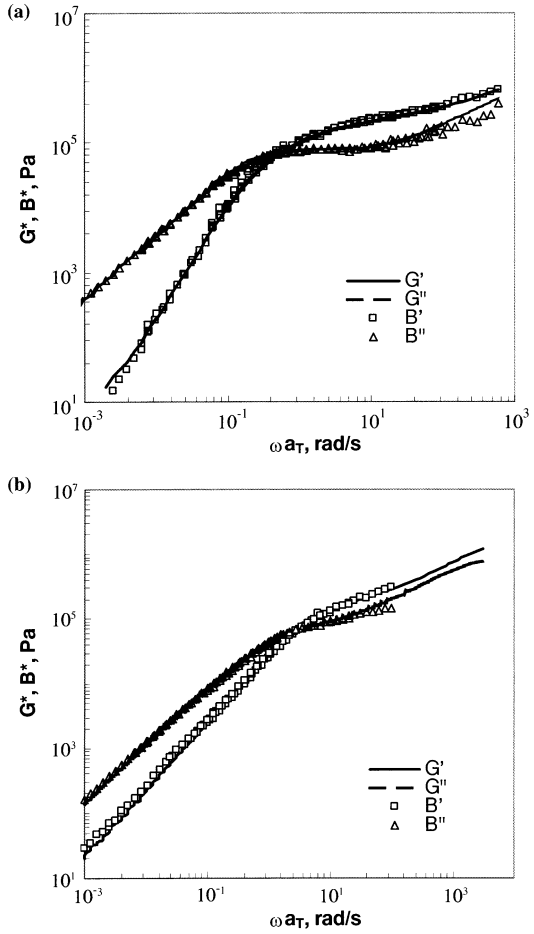

Figure 5. SOR for (a) 8-arm-45K-star and (b) 20K-HBPS. Solid and dashed lines represent viscoelastic moduli G' and G'', and symbols, corresponding components of shear stress (B' and B'') obtained from the birefringence data.

the symmetric star with longest arms (8-arm-45K-star) (Figure 6a). On the basis of this, it is reasonable to elucidate that short arms of the star cause the stress−optical coefficient of this polymer to be similar to the unentangled linear PS with comparable MW discussed above. In fact, the C of 8-arm-10K symmetric star is close to that of 13K-L-PS (Table 1). In linear and symmetric stars, for an arm molecular weight significantly lower than 20 000, the stress−optical rule is obeyed, but the absolute value of the stress−optic coefficient is lower.

In contrast, moderately branched HBPS with weakly entangled branches showed distinctly different stress−optical behavior compared to linear polymers and symmetric stars. Over the wide frequency and temperature range 20K-HBPS and 50K-HBPSappear to obey the stress−optical rule. Figure 5b demonstrates this for 20K-HBPS, where G^* and B^* calculated from the mechanical stress and optical birefringence, respectively, are in good agreement. Note that these HBPS possess the highest branch molecular weight, and the density of their branches is only moderate (Table 1). The temperature dependence of C for 20K-HBPS and 50K-HBPS as a function of frequency is shown in Figure 6b. In this case, both HBPS have sufficiently long branches in order to comply with the theory of elasticity. However, in the region where the SOR holds, their C is found to be ∼30% lower than the corresponding value for linear polystyrene of the same total molecular weight or even of the chain length of twice the branch length of HBPS

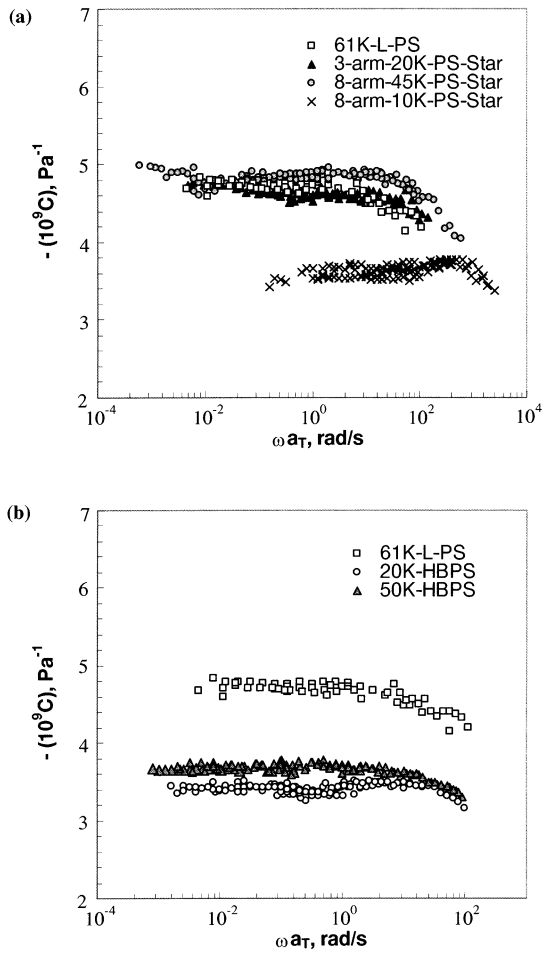

Figure 6. Temperature dependence of C: (a) symmetric PS stars; (b) moderately branched HBPS.

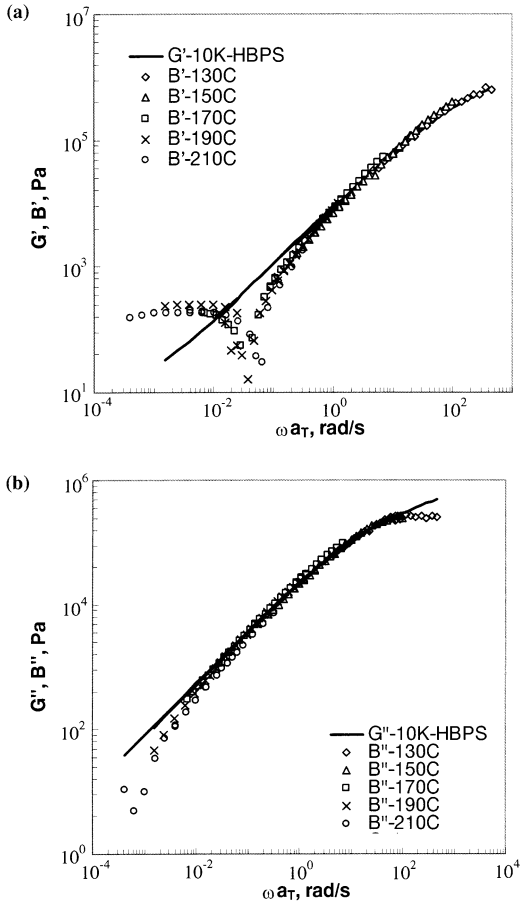

Figure 7. Failure of the SOR for 10K-HBPS seen in the (a) in-phase birefringence B' and the (b) out-of-phase birefringence B''. Solid lines represent mechanical moduli G' and G'', and symbols, corresponding components of shear stress (B' and B'') obtained at different temperatures from the birefringence data.

(Table 1). Therefore, such differences between the C of 20K-HBPS and 50K-HBPS and the C of 3-arm-20K-star and 8-arm-45K-star could be due to the relatively higher branch density of these HBPS.

Densely Branched HBPS. When the branch density is high and the branches are short, which is the case for 10K-HBPS, a clear *breakdown* of SOR is observed, even though it is a homopolymer melt (Figure 7). To compare the different polymers, we calculate the stress−optical ratio, so that the intrinsic birefringence contribution is "as appropriately normalized" as possible. We note that, for the 5K- and the 10K-HBPS, even the G^* data show the contributions from the additional mode. Therefore, the strong frequency dependence of stress−optical ratio can be thought of as a factor that reflects sensitivity of birefringence to the "structural" contributions, beyond that shown by G^*. The breakdown is especially pronounced *at low frequencies*, suggesting that the stress−optical ratio of this polymer is no longer frequency independent. At high frequencies the corresponding components of G^* and B^* overlap quite well, especially for 10K-HBPS. We then used the C obtained in this dynamic range to subsequently calculate the in-phase (B') and out-of-phase (B'') components of birefringence, and compare them to the corresponding components of stress G' and G'', respectively. At low frequencies, the elastic part B' of 10K-HBPS showed a significant deviation from G'. Besides the strong dependence on frequency, the C of this polymer appears to change the sign. For linear PS, the sign of C is defined by the intrinsic polarizability of a monomer unit (eq 2) and is negative. For the densely branched HBPS, it is negative at high frequencies (as is the case for linear PS), but becomes positive at lower frequencies. Since logarithmic axes were used, the change of sign can be seen through the occurrence of the minima in B' and B''. The character of failure of the SOR in our work is consistent with the previous studies on block copolymers.[54] However, such failure for homopolymer melts is highly unusual and reflects the complex architectural contributions to birefringence, in a disproportionate manner compared to stress.

The change in sign of C of 10K-HBPS is gradual, for B' and B'' show upturns at 0.04 and 0.0006 rad/s, respectively. The frequency at which either B' or B'' reverses the sign is distinct, and the data from different temperatures agree well when plotted on a master curve (Figure 7). In Figure 9a, we plot the normalized in-phase ($C' = B'/G'$) and out-of-phase ($C'' = B''/G''$) components of C for 10K-HBPS. At high frequencies, these normalized ratios are approximately equal, with an estimated value of -1, which suggests that the SOR is valid. The actual magnitude of C in this range is equal to -2.5×10^{-9} Pa^{-1}, which is significantly lower than C of a linear PS of comparable total molecular weight, and is even lower than the C of 13K-L-PS. This effect is similar to a decrease in C for moderately branched 20K-HBPS and 50K-HBPS discussed above. As seen from the figure, with decreasing frequency, C' increases much stronger than C''.

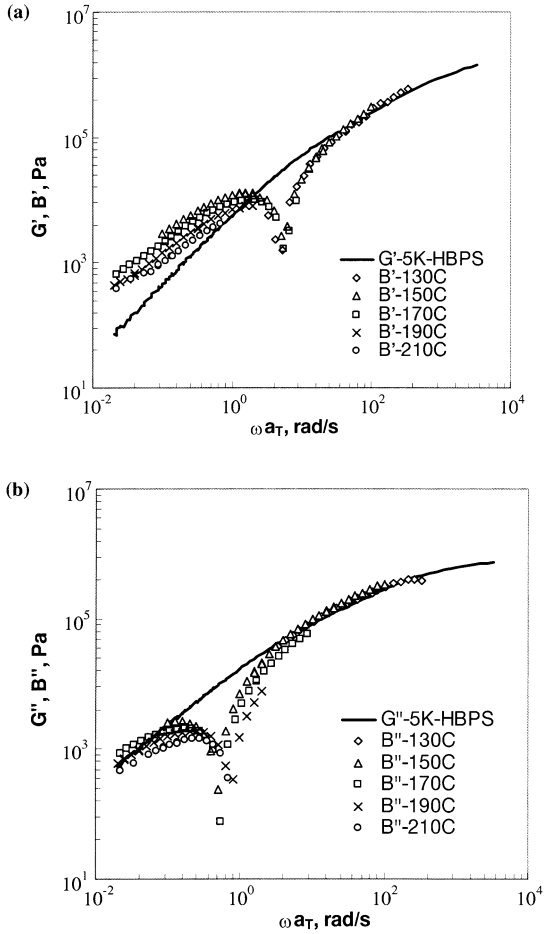

Figure 8. Failure of the SOR for 5K-HBPS seen in the (a) in-phase birefringence B' and the (b) out-of-phase birefringence B''. Solid lines represent mechanical moduli G' and G'', and symbols, corresponding components of shear stress (B' and B'') obtained at different temperatures from the birefringence data.

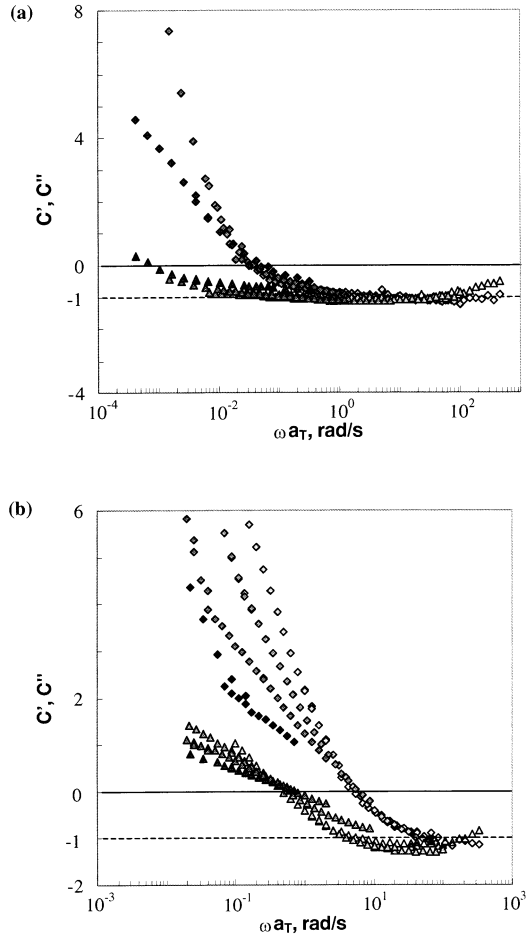

Figure 9. Frequency dependence of the normalized in-phase ($C' = B'/G'$, shown by rhombs) and out-of-phase ($C'' = B''/G''$, shown by triangles) components of C: (a) 10K-HBPS; (b) 5K-HBPS. $T_{ref} = 150$ °C. Note that the darker shade of the symbol corresponds to a higher experimental temperature (i.e., T = 130 °C is shown by open symbol, and T = 210°C, by black shade).

Even more convincing failure of the SOR is observed when flow birefringence measurements involved 5K-HBPS. This polymer has the shortest branches and a comparable branch density to that of 10K-HBPS. We found that for 5K-HBPS the SOR would experience total breakdown even at higher frequencies (Figure 8). The upturn in B' for 5K-HBPS already occurs at $\omega = 5.4$ rad/s and in B'' at about 0.54 rad/s. As was the case for 10K-HBPS, the frequency at which either B' or B'' changes sign is also very distinct. The total change of sign of the C from negative to positive corresponds to $\omega = 0.54$ rad/s. On the basis of the few data at the highest frequencies, an estimated value of $C \approx -1.6 \times 10^{-9}$ Pa^{-1} was obtained. This number is also substantially lower than that of the linear polymer of comparable branch length, 5K-L-PS (Table 1). When plotting normalized ratios C' and C'' of 5K-HBPS, strong frequency dependence is observed (Figure 9b). Comparing the effect of branch length on the flow birefringence of HBPS having similar branch density, it is evident that as the molecular weight of the branch decreases, the change of sign occurs at a higher frequency (0.54 rad/s for 5K-HBPS as opposed to 0.0006 rad/s for 10K-HBPS). The magnitude of the observed *form* effects is also much stronger for 5K-HBPS. In summary, the rheo-optical data suggest that as the branch density increases, there is an increasingly complex breakdown of the SOR.

Discussion

Our results can be discussed further by considering the effect of branch density on the rheology and orientation behavior, and the role of entanglement on the manifestation of this effect. When the branch density is relatively low ($\sim$<20), the rheology and the flow birefringence are qualitatively and almost quantitatively similar, provided the branch lengths are comparable. This is seen through the comparison of the temperature dependence of G^* and the shift factor (a_T) of 8-arm-45K-star with 50K-HBPS (with $\sim$20 branches), and the 3-arm-20K-star and 61K-L-PS. Previous studies suggest that properties of an entangled symmetric star would be governed only by the molecular weight of an arm.[9,48] However, as seen from Figure 6b, the stress−optical coefficient of the 50K-HBPS ($\approx -3.7 \times 10^{-9}$ Pa^{-1}) is appreciable lower in magnitude than that of the 8-arm-45K−PS ($\approx -4.85 \times 10^{-9}$ Pa^{-1}), suggesting that the flow birefringence is already sensitive to the conformational change going from 8 to 20 arms.

As the branch density increases and the arm molecular weight decreases, the nonterminal behavior and the breakdown of the SOR become more pronounced. Quantitative measurements of such breakdown can therefore be an effective tool to study contributions from different length scales in complex polymeric materials

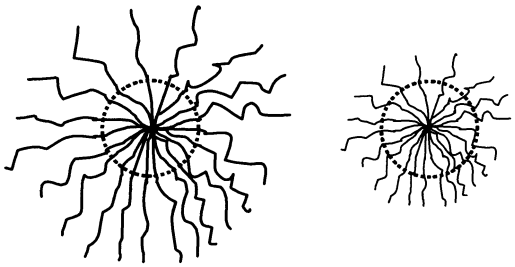

Figure 10. Schematic representation of the formation of "core−shell" morphology: (a) 10K-HBPS; (b) 5K-HBPS. Note that the ratio of shell to core volume is smaller for 10K-HBPS than it is for 5K-HBPS.

as well as to potentially quantify the degree of branching density. For example, in lamellar diblock copolymers, nonuniform contributions to stress and birefringence from nanostructural orientation caused SOR to fail, analogous to the observations of strong frequency dependence of C in our study.[54] At high frequencies, segmental contributions dominate the birefringence and the stress of HBPS. At lower frequencies, relaxation modes become more important. In the case of a lamellar diblock copolymer, it was the lamellar nanostructure, and the stress−optical coefficient showed a strong low-frequency response. Analogous SOR breakdowns have also been used to infer component orientations in miscible blends. The interesting aspect of the current work is the fact that this failure is being seen in a *homopolymer* melt.

In our study, the development of nonterminal behavior is also found for all HBPS with the branching density higher than about 20 branches. The homopolymer HBPS with the highest branch number (5K-HBPS and 10K-HBPS) showed distinct thermal properties and clearly nonterminal rheology, but also they no longer followed the stress−optical rule. For 5K-HBPS and 10K-HBPS, it appears that the additional contributions have origins in high branch density. Therefore, there may be some crowding of the chain segments near the center, leading to preferential radial orientation. This could produce a "core" formation, connected to a "shell" (Figure 10). In earlier work, the "core−shell" morphology was observed in highly entangled, multiarm hyperstar polybutadienes and polyisoprenes, using rheology, solution viscometry, Monte Carlo simulations, SANS and SAXS measurements.[35,38] In fact, X-ray scattering confirmed that for the same number of arms of a symmetric star, the magnitude of scattering intensity was proportional to the concentration of star centers per unit volume and center-to-center correlation distance. This was also suggested by McLeish and Milner in highly dense stars.[13] Such organization into the "ordered liquid state" would produce a length scale that is larger than the entanglement length.

The core−shell structure may give rise to a density contrast, which would lead to a refractive index contrast, producing, in turn, a "form" contribution to the birefringence. This is somewhat analogous to what is seen in block copolymers. The positive form contribution may be in competition with the negative intrinsic contribution arising from the segmental/chain orientation. At high frequencies, the intrinsic contribution to birefringence and stress dominates the form part. Whereas, at low frequencies the intrinsic contributions largely relax, leading to the birefringence being dominated by the "form" effects. The "form" effect may be constant with frequency, but the stress decreases with decreasing frequency, leading to a sharp increase in the stress−optic coefficient. For a given branch density, this would suggest that the "form" factor would be more dominant in the 5K-HBPS, since its shell is of much smaller size than that of the 10K-HBPS, as seen from the hypothetical representation of the core−shell morphology in Figure 10. The "core" size may be comparable, since both have approximately the same number of arms. This leads to a greater (or "stronger") failure of the SOR for the 5K-HBPS. In addition, the smaller the size of such HBPS, the greater is the magnitude of this failure. For 10K-HBPS the SOR failure starts at a much lower frequency (∼1 rad/s), whereas for 5K-HBPS it occurs at 20 rad/s (as estimated from the highest frequency where the G' and B' start to deviate). Also, in these unentangled melts, the "form" birefringence contribution from the core is more readily evident, since the entanglement effects are largely absent. Our results suggest that the tendency of the chains to preferentially orient near the branch point may have an effect even when there are only 20 branches. The "net" positive form contribution may be the cause for the reduced stress−optical coefficient of 50K-HBPS (∼20 arms) compared to the 8-arm-45K symmetric star. This core−shell structure could manifest itself in unusual ways in blends of these polymers with linear PS, and other homopolymers, where branch density may cause "molecular-scale" phase separation, even though linear blends would be miscible. These are currently under investigation.

Conclusions

Simultaneous rheo-optical measurements on polymers of different molecular architectures, such as symmetric PS stars and starlike HBPS melts, allowed us to get a better understanding of the microscopic origins responsible for unusual dynamics of HBPS seen in rheology, solution and thermal properties, and flow birefringence. Studying unentangled or weakly entangled melts permitted obtaining a better glimpse of the role of branch density. Our results suggest the following.

(1) Nonterminal response of HBPS may be correlated with the branch density. As the density increases, the nonterminal behavior becomes more pronounced. Such behavior points out at the existence of the additional slow relaxation modes.

(2) Linear PS and symmetric PS stars with three and eight arms seem to obey the SOR in the wide range of frequency and temperature. When the molecular weight (or arm molecular weight of a star) is lower than ∼20 000, the magnitude of C is reduced.

(3) When the branch density increases (HBPS with moderate branching density in the range of about 20−30), there is a hint of low-frequency nonterminal behavior, but the stress−optical rule still holds. However, C is lower by ∼30%, compared to L-PS and symmetric stars.

(4) When the branch density is "high" (as in 5K- and 10K-HBPS with ∼50 branches), there may be a core−shell structure, formed by the preferential radial orientation of chain segments near the central branch point. The core−shell structure could have a positive "form" contribution to the birefringence, which is more easily manifested at low frequencies, when the intrinsic

contributions have largely relaxed. These unusual stress−optic behavior is more evident in the high branch density, low arm molecular weight melts, which would have a relatively large core compared to the shell.

(5) The additional contributions to polymer relaxation coming from the formation of core−shell structure are predominantly of the elastic nature (evident from the in-phase G', B', and C' behavior) compared to those corresponding to out-of-phase components. The suggestion of core−shell structure in these materials is consistent with previous studies on highly entangled hyperstars. The flow birefringence studies will be augmented in the future with light scattering. Role of branch architecture on the miscibility, rheological, and mechanical properties of blends is being explored.

Acknowledgment. Funding from NSF (R.M.K.) (CAREER Award DMR-#9876221), 3M non-tenured faculty grant (R.M.K.), and WSU-Institute of Manufacturing Research (Graduate Research Assistantship for S.B.K.) are greatly appreciated.

References and Notes

(1) Ferry, J. D. *Viscoelastic Properties of Polymers*; John Wiley & Sons: New York, 1980.
(2) Dealy, J. M.; Wissbrun, K. F. *Melt Rheology and Its Role in Plastics Processing: Theory and Applications*; Chapman & Hall: New York, 1990.
(3) Kharchenko, S. B.; Kannan, R. M.; Cernohous, J. J.; Venkataramani, S. Role of Architecture on the Rheology and Orientation Behavior of Linear, Star, and Hyperbranched Polymer Melts. 1. Synthesis and Molecular Characterization. *Macromolecules* **2003**, *36*, 399.
(4) Ball, R. C.; McLeish, T. C. B. *Macromolecules* **1989**, *22*, 1911. McLeish, T. C. B.; Oconnor, K. P. *Makromol. Chem. Macromol. Symp.* **1992**, *56*, 127.
(5) de Gennes, P.-G. *J. Phys.* **1975**, *36*, 1199.
(6) Doi, M.; Kuzuu, N. Y. *J. Polym. Sci., Polym. Lett. Ed.* **1980**, *18*, 775.
(7) Pearson, D. S.; Helfand, E. *Macromolecules* **1984**, *17*, 888.
(8) Doi, M.; Edwards, S. F. *The Theory of Polymer Dynamics*; Clarendon Press: Oxford, England, 1986.
(9) Graessley, W. W. *Macromolecules* **1982**, *15*, 1164. Graessley, W. W.; Raju, V. R. *J. Polym. Sci., Polym. Symp.* **1984**, *71*, 77. Carella, J. M.; Gotro, J. T.; Graessley, W. W. *Macromolecules* **1986**, *19*, 659.
(10) Larson, R. *Constitutive Equations for Polymer Melts and Solutions*; Butterworths: Boston, MA, 1988.
(11) McLeish, T. C. B.; Allgaier, J.; Bick, D. K. *Macromolecules* **1999**, *32*, 6734.
(12) Roovers, J.; Comantia, B. *Adv. Polym. Sci.* **1999**, *142*, 179.
(13) McLeish, T. C. B.; Milner, S. T. *Adv. Polym. Sci.* **1999**, *143*, 195.
(14) Daniels, D. R.; McLeish T. C. B.; Kant, R.; Crosby, B. J.; Young, R. N.; Pryke, A.; Allgaier, J.; Groves, D. J.; Hawkins, R. *J. Rheol. Acta* **2001**, *40*, 403.
(15) Larson, R. G. *Macromolecules* **2001**, *34*, 4556.
(16) Charlesby, A. J. *J. Polym. Sci.* **1955**, *17*, 370. Vinogradov, G. V.; Malkin, A. Ya. *Rheology of polymers: viscoelasticity and flow of polymers*; Mir: Moscow; Springer-Verlag: Berlin and New York: 1980. Fujimoto, T.; Narukawa, H.; Nagasawa, M. *Macromolecules* **1970**, *3*, 57.
(17) Ball, R. C.; McLeish, T. C. B. *Macromolecules* **1989**, *22*, 1911. Yurasova, T. A.; McLeish, T. C. B.; Semenov, A. N. *Macromolecules* **1994**, *27*, 7205.
(18) Milner, S. T.; McLeish, T. C. B. *Macromolecules* **1997**, *30*, 2159.
(19) Blottière, B.; McLeish, T. C. B.; Hakiki, A.; Young, R. N.; Milner, S. T. *Macromolecules* **1998**, *31*, 9295.
(20) Pattamaprom, C; Larson, R. G; Van Dyke, T. *J. Rheol. Acta* **2000**, *39*, 517.
(21) Frischknecht AL, Milner ST. *Macromolecules* **2000**, *33*, 9764.
(22) Fukuda, M.; Osaki, K.; Kurata, M. *J. Polym. Sci., Polym. Phys.* **1975**, *13*, 1563.
(23) Huber, K.; Burchard, W.; Fetter, L. J. *Macromolecules* **1984**, *17*, 541.
(24) Fetters, L. J.; Lohse, D. J.; Richter, D.; Witten, T. A.; Zirkel, A. *Macromolecules* **1994**, *27*, 4639.
(25) Kasehagen, L. J.; Macosko, C. W. *J. Rheol.* **1998**, *42*, 1303. Read, D. J.; McLeish, T. C. B. *Macromolecules* **2001**, *34*, 1928.
(26) Wood-Adams, P. M.; Dealy, J. M. *Macromolecules* **2000**, *33*, 7481.
(27) Bin Wadud, S. E.; Baird, D. G. *J. Rheol.* **2000**, *44*, 1151.
(28) Malmberg, A.; Gabriel, C.; Steffl, T.; Münstedt, H.; Lofgren, B. *Macromolecules* **2002**, *35*, 1038. Gabriel, C.; Münstedt, H. *Rheol. Acta* **2002**, *41*, 232.
(29) Tomalia, D. A.; Baker, H.; Dewald, J.; Hall, M.; Kallos, G.; Martin, S.; Roech, J.; Ryder, J.; Smith, J. *Polym. J.* **1985**, *17*, 177. Hawker, C. J.; Frechet, J. M. J. *J. Am. Chem. Soc.* **1990**, *112*, 7638. Mourey, T. H.; Turner, S. R.; Rubinstein, M.; Frechet, J. M. J.; Hawker, C. J.; Wooley, K. L. *Macromolecules* **1992**, 25, 2401. Malmstrom, E.; Hult, A. *J. Macromol. Sci.—Rev. Macromol. Macromol. Chem. Phys.* **1997**, *37*, 555. Hult, A.; Johansson, M.; Malmström, E. *Adv. Polym. Sci.* **1998**, *143*, 1.
(30) Uppuluri, S.; Keinath, S. E.; Tomalia, D. A.; Dvornic, P. R. *Macromolecules* **1998**, 31, 4498. Hawker, C. J.; Farrigton, P. J.; Mackay, M. E.; Wooley, K. L.; Frechet, J. M. J. *J. Am. Chem. Soc.* **1995**, *117*, 4409. Simon, P. F. W.; Muller, A. H. E.; Pakula, T. *Macromolecules* **2001**, *34*, 1677.
(31) Ferri, D.; Lomellini, P. *J. Rheol.* **1999**, *43*, 1355.
(32) Robertson, C. G.; Roland, C. M. *J. Rheol.* **2002**, *46*, 307.
(33) Rubinstein, M.; Helfand, E.; Pearson, D. S. *Macromolecules* **1987**, *20*, 822.
(34) Roovers, J.; Zhou, L. L.; Toporowski, P. M.; Van Der Zwan, M.; Iatrou, H.; Hadjichristidis, N. *Macromolecules* **1993**, *26*, 4324.
(35) Vlassopoulos, D.; Pakula, T.; Fytas, G.; Roovers, J.; Karatasos, K.; Hadjichristidis, N. *Europhys. Lett.* **1997**, *39*, 617. Pakula, T.; Vlasopoulos, D.; Fytas, G.; Roovers, J. *Macromolecules* **1998**, *31*, 8931.
(36) Hatzikiriakos, S. G. *Polym. Eng. Sci.* **2000**, *40*, 2279.
(37) Wood-Adams, P.; Costeux, S. *Macromolecules* **2001**, *34*, 6281.
(38) Roovers, J. *Macromol. Symp.* **1997**, *121*, 89.
(39) Janeschitz-Kriegl, H. *Polymer Melt Rheology and Flow Birefringence*; Springer-Verlag: Berlin and New York, 1983.
(40) Johnson, S. J.; Frattini, P. L.; Fuller, G. G. *J. Colloid Interface Sci.* **1985**, *104*, 440.
(41) Kharchenko, S. B.; Kannan, R. M.; Cernohous, J. J.; Venkataramani, S.; Babu, G. N. *J. Polym. Sci., Part B: Polym. Phys.* **2001**, *39*, 2562.
(42) Raju, V. R.; Rachapudy, H.; Graessley, W. W. *J. Polym. Sci., Polym. Phys.* 1979, 17, 1223. Gell, C. B.; Graessley, W. W.; Efstratiadis, V.; Pitsikalis, M.; Hadjichristidis, N. *J. Polym. Sci., Part B: Polym. Phys.* **1997**, *35*, 1943.
(43) Sendijarevic, I.; Liberatore, M. W.; McHugh, A. J. *J. Rheol.* **2001**, *45*, 1245.
(44) Cohen, M. H.; Turnbull, D. *J. Chem. Phys.* **1959**, *11*, 1164.
(45) Plazek, D. J.; O'Rourke, V. M. *J. Polym. Sci., Part A-2.* **1971**, *9*, 209.
(46) Roovers, J. *Macromolecules* **1985**, *18*, 1359.
(47) Wood-Adams, P. M.; Dealy, J. M.; deGroot, A. W.; Redwine, O. D. *Macromolecules* **2000**, *33*, 7489. Hingmann, R.; Marczinke, B. L. *J. Rheol.* **1994**, *38*, 573. Koopmans, R. J. *SPE ANTEC Technol. Pap.* **1997**, *43*, 1006.
(48) Struglinski, M. J.; Graessley, W. W.; Fetters, L. J. *Macromolecules* **1988**, *21*, 783.
(49) Nunez, C. M.; Chiou, B. S.; Andrady, A. L.; Khan, S. A. *Macromolecules* **2000**, *33*, 1720.
(50) Sendijarevic, I.; McHugh, A. *Macromolecules* **2000**, *33*, 590.
(51) Han, C. D.; Drexler, L. H. *J. Appl. Polym. Sci.* **1973**, *17*, 329. Retting, W. *Colloid Polym. Sci.* **1979**, *257*, 689. Muller, R.; Froelich, D. *Polymer* **1985**, *26*, 1477. Venerus, D. C.; Zhu, S.-H.; Ottinger, H. C. *J. Rheol.* **1999**, *43*, 795.
(52) Inoue, T.; Onogi, T.; Yao, M.-L.; Osaki, K. *J. Polym. Sci., Part B: Polym. Phys.* **1999**, *37*, 389.
(53) Kornfield, J. A.; Verma, R. K. *Proc. XIIIth International Congress on Rheology*; Cambridge, U.K., 2000; 1, 281.
(54) Kannan, R. M.; Kornfield, J. A. *J. Rheol.* **1994**, *38*, 1127.

MA025649Y